Regulation of polarized growth initiation and termination cycles by the polarisome and Cdc42 regulators

Scott Bidlingmaier[1] and Michael Snyder[1,2]

[1]Department of Molecular Biophysics and Biochemistry and [2]Department of Molecular, Cellular, and Developmental Biology, Yale University, New Haven, CT 06520

The dynamic regulation of polarized cell growth allows cells to form structures of defined size and shape. We have studied the regulation of polarized growth using mating yeast as a model. Haploid yeast cells treated with high concentration of pheromone form successive mating projections that initiate and terminate growth with regular periodicity. The mechanisms that control the frequency of growth initiation and termination under these conditions are not well understood. We found that the polarisome components Spa2, Pea2, and Bni1 and the Cdc42 regulators Cdc24 and Bem3 control the timing and frequency of projection formation. Loss of polarisome components and mutation of Cdc24 decrease the frequency of projection formation, while loss of Bem3 increases the frequency of projection formation. We found that polarisome components and the cell fusion proteins Fus1 and Fus2 are important for the termination of projection growth. Our results define the first molecular regulators that control the timing of growth initiation and termination during eukaryotic cell differentiation.

Introduction

The ability to polarize cell growth in response to internal and/or external cues is a fundamental property of almost all cell types. The precise regulation of the timing of growth initiation and termination is critical for the formation of cellular structures of distinct sizes and shapes that are important for many biological processes. For example, cell motility, axonal guidance, nutrient absorption by the microvilli of epithelial cells, and plant fertilization require polarized cell structures whose growth is dynamic and precisely regulated (Heintzelman and Mooseker, 1992; Bedinger et al., 1994; da Silva and Dotti, 2002; Pollard and Borisy, 2003). In the case of mating projection formation described in the next section, polarized cell growth occurs in an oscillatory pattern in which polarized projections form, grow, and then later cease growth. How the timing of polarized cell growth initiation occurs is not well understood, and almost no attention has been devoted to understanding polarized growth termination.

The budding yeast *Saccharomyces cerevisiae* initiates polarized growth from the cell surface at several stages of its life cycle and is a useful organism for understanding the regulation of polarized growth events. During vegetative growth, the G1 Cdk complex (Cln-Cdc28) promotes bud emergence (Lew and Reed, 1993). Growth is initially restricted to the bud tip (apical growth) until rising activity of mitotic Cdk complexes (Clb-Cdc28) induces growth throughout the bud surface (Lew and Reed, 1993). During mating, haploid cells respond to pheromone produced by cells of the opposite mating type and form specialized structures called mating projections that are important for cell–cell recognition. Growth is restricted to the projection tip and oriented along a pheromone gradient, allowing cells to seek out mates and then fuse with them (Jackson and Hartwell, 1990; Segall, 1993).

In the presence of a high concentration of mating pheromone, cells initiate and terminate projection growth in regular cycles (Bucking-Throm et al., 1973). This phenomenon is thought to enable cells to locate nearby partners and fuse (see Discussion). A similar phenomenon also occurs in budding cells; when the activity of the mitotic Clb-Cdc28 kinase is shut off, cells arrest and periodically form buds that grow to a defined length (Goebl et al., 1988; Schwob et al., 1994; Mathias et al., 1996; Chun and Goebl, 1997). Interestingly, these periodic initiations of polarized growth occur independently of the major budding yeast cell cycle–regulating Cdk,

Figure 1. **Periodic mating projection initiation and termination in wild-type cells treated with high concentration of pheromone.** (A) Unsynchronized exponentially growing wild-type cells were incubated with 5 μg/ml α-factor, and projection emergence was analyzed as a function of time. At least 100 cells were analyzed for each time point, and the data represent the average of two independent experiments. (B) Time-lapse analysis of pheromone-treated wild-type cells. Wild-type cells were grown on YPAD/agarose pads (see Materials and methods) in the presence of 5 μg/ml α-factor. A representative cell is shown. Arrows mark the emergence of a new projection. Bar, 1.5 μm. (C) Examples of projection growth rates for two cells. Projection growth was monitored at 10-min intervals, and the 30-min moving average growth rate for each projection (first or second) was plotted. Plots begin after the initiation of the first projection.
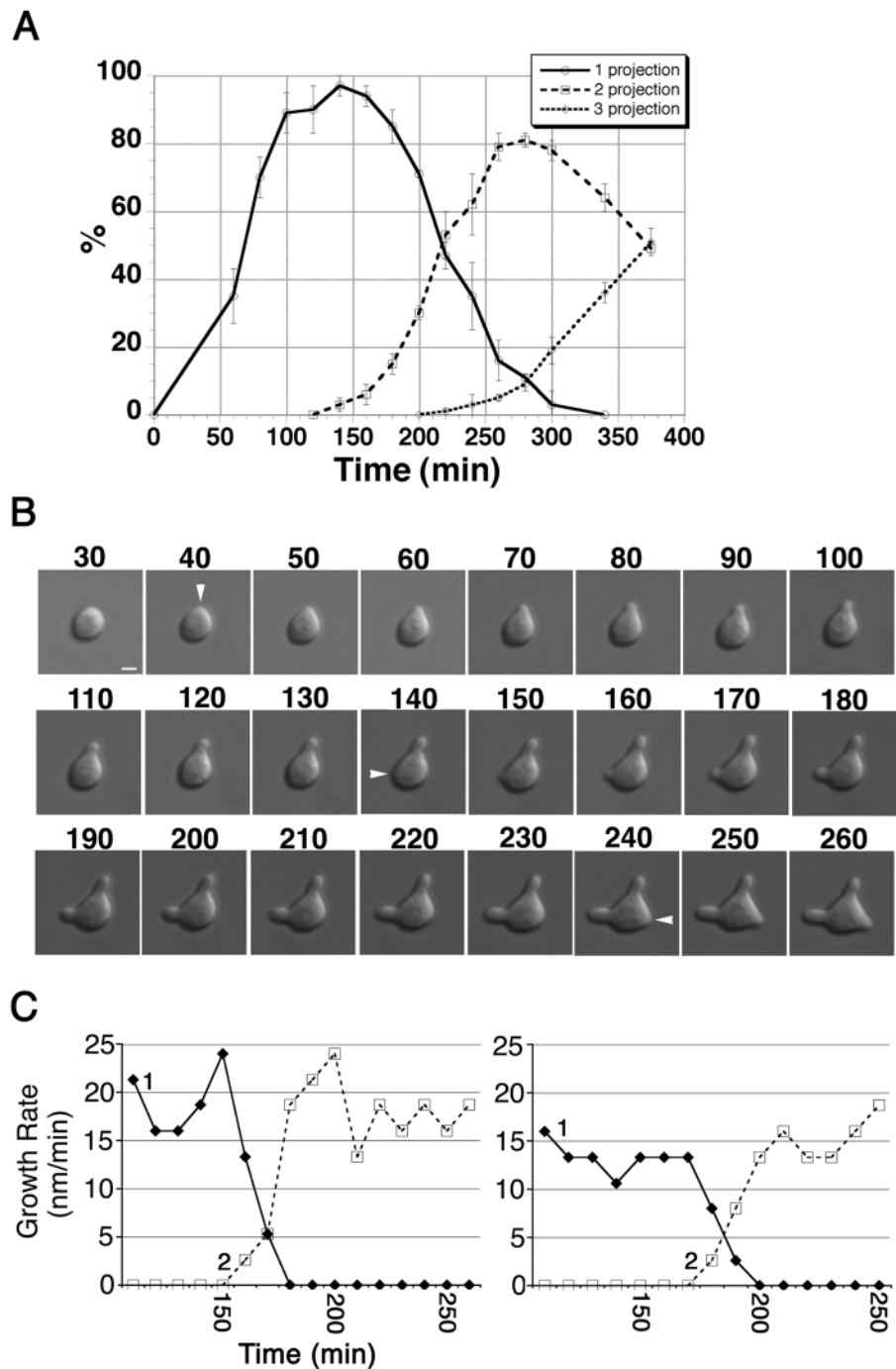
Cdc28 (Haase and Reed, 1999). The biochemical nature of the oscillator that triggers the periodic initiation and termination of polarized growth in these cases is unknown.

During both budding and mating projection formation, polarization of the actin cytoskeleton drives the initiation of polarized growth sites (Madden and Snyder, 1998; Pruyne and Bretscher, 2000). Local activation of the essential rho-related GTPase Cdc42 is critical for the initiation of actin polarization. In the absence of Cdc42 activity, cells continue to grow isotropically, becoming large and round. Cellular Cdc42 dynamically cycles between the inactive GDP-bound form and the active GTP-bound form. The cycling of Cdc42 is regulated by the essential guanine nucleotide ex-

change factor (GEF) Cdc24 (Zheng et al., 1994) and the GTPase-activating proteins (GAPs) Bem3, Rga1, and Rga2 (Smith et al., 2002). Cdc42 is believed to signal through multiple effectors that preferentially interact with GTP-bound Cdc42. These include the PAK-like kinases Ste20 and Cla4, two related proteins, Gic1 and Gic2, and the formin homologue Bni1 (Johnson, 1999).

Bni1 localizes to sites of polarized growth (Evangelista et al., 1997; Fujiwara et al., 1998) and is important for the assembly of actin cables (Evangelista et al., 2002; Sagot et al., 2002), which are thought to direct organelle segregation and the polarized delivery of secretory vesicles and specific mRNAs to the cell surface (Bretscher, 2003). *bni1Δ* cells

have defects in bud emergence, mating projection formation, and diploid bud site selection (Zahner et al., 1996; Evangelista et al., 1997; Ozaki-Kuroda et al., 2001). Bni1 has a homologue in yeast, Bnr1, and the simultaneous disruption of Bni1 and Bnr1 prevents cells from establishing polarity (Evangelista et al., 2002). The efficient activation and localization of Bni1 requires Spa2 and Pea2 (Fujiwara et al., 1998; Ozaki-Kuroda et al., 2001; Sagot et al., 2002). Spa2 and Pea2 localize to sites of polarized growth, and *spa2Δ* and *pea2Δ* cells have polarized growth defects that are similar to those observed in *bni1Δ* cells (Snyder, 1989; Gehrung and Snyder, 1990; Snyder et al., 1991; Chenevert et al., 1994; Valtz and Herskowitz, 1996). Multiple physical interactions have been detected between Bni1, Spa2, Pea2, and Bud6, and they have been proposed to act together as a complex termed the polarisome (Evangelista et al., 1997; Fujiwara et al., 1998; Sheu et al., 1998).

In this report, we have investigated the mechanisms that regulate mating projection formation and termination and the frequency of these events in haploid yeast cells treated with a high concentration of pheromone. Our results suggest that the Cdc42 regulator Bem3 and the polarisome components Spa2 and Pea2 act upstream of Bni1 to regulate the timing of mating projection formation. Surprisingly, we found that polarisome components as well as the cell fusion proteins Fus1 and Fus2 are important for termination of projection growth and delocalization of actin. Moreover, Fus1 does not regulate the timing of mating projection formation, suggesting that initiation and termination of growth are regulated by partially separate pathways. Our results define the first molecular regulators controlling the timing of periodic mating projection formation and growth termination in budding yeast and provide insight into the mechanisms of dynamic regulation of polarized growth in eukaryotes.

Results

Periodic mating projection initiation and termination occurs in wild-type cells treated with a high concentration of pheromone

We first characterized periodic mating projection initiation in wild-type cells using our strain background. Unsynchronized cells were incubated with α-factor, and projection formation was monitored as a function of time for 375 min (Fig. 1 A). The time at which 50% of the cells had formed one projection was 67 min (Fig. 1 A). The average interval between the initiation of the first and second mating projections was 143 min, and the average interval between the initiation of the second and third projections was similar, 130 min (Fig. 1 A). The overall average time per projection initiation (initiation period) was 119 ± 4 min. The average rate of total projection growth was 16.1 ± 0.8 nm/min.

To more precisely characterize the morphological response to pheromone, we directly observed living pheromone-treated cells using time-lapse microscopy. Similar to what we observed for the asynchronous population, the average time at which cells formed their first projection was 65 ± 18 min ($n = 17$), and the average period between the initiation of the first and the second projections was 120 ± 33 min (Fig. 1 B; $n = 15$). There was no difference in the
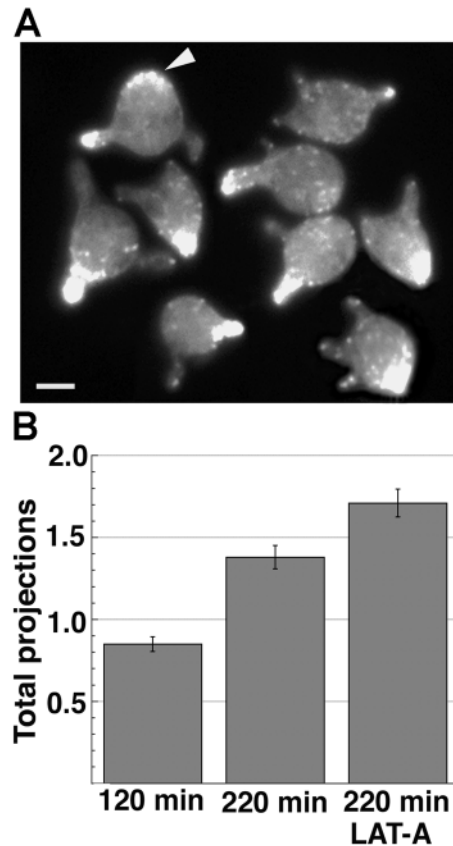

Figure 2. **The relationship between projection initiation and termination.** (A) Wild-type cells were incubated with α-factor for 6 h and stained for F-actin. The arrow identifies a cell with two polarized actin sites. Bar, 3.0 μm. (B) Wild-type cells were incubated with α-factor for 120 min and then treated with Lat-A to transiently disrupt the actin cytoskeleton. Cells were returned to growth in the presence of α-factor for 100 min, and the number of total projections formed was compared with mock-treated cells. At least 100 cells were analyzed for each time point and the data represent the average of two independent experiments.

growth rate of first and second projections (17.8 ± 2.6 nm/min and 18.0 ± 2.3 nm/min, respectively; $n = 8$).

Our time-lapse observations of pheromone-treated wild-type cells revealed three features not previously reported. First, visible growth of existing projections stopped at approximately the same time or slightly after the emergence of a new projection (Fig. 1, B and C). Growth of the first projection terminated an average of 11.0 ± 7.4 min after the initiation of the second projection ($n = 11$). Second, projections that ceased growth were never observed to resume growth (Fig. 1, B and C). Third, projections grew to approximately the same length (within 20%) before terminating growth.

To more precisely investigate the correlation between the termination of previous projection growth sites and the formation of new projections, we treated wild-type cells with α-factor for 6 h and then examined the actin cytoskeleton; polarized actin patches accumulate at active growth sites and are visible before projection growth (Gehrung and Snyder, 1990). After a 6-h incubation with α-factor, cells had an average of 2.96 ± 0.10 mating projections, and all cells had at least two projections. $90.6 \pm 0.6\%$ of cells had exactly one site of polarized actin, and $9.4 \pm 0.6\%$ had two sites of polarized actin

Figure 3.   **Deletion of *SPA2*, *PEA2*, or *BNI1* decreases the frequency of periodic mating projection initiation.** (A) Unsynchronized exponentially growing *spa2Δ* cells were incubated with α-factor, and projection emergence was analyzed as a function of time. At least 100 cells were analyzed for each time point and the data represent the average of two independent experiments. (B) Time-lapse analysis of pheromone-treated *spa2Δ* cells. *spa2Δ* cells were grown on YPAD/agarose pads (see Materials and methods) in the presence of α-factor. A representative cell is shown. Arrows mark the emergence of a new projection. Area outlined by white line represents growth that occurred in the first projection after the initiation of the second projection. Bar, 1.5 μm. (C) Examples of projection growth rate for two *spa2Δ* cells. Projection growth was monitored at 10-min intervals, and the 30-min moving average growth rate for each projection (first or second) was plotted. Plots begin after the initiation of the first projection.
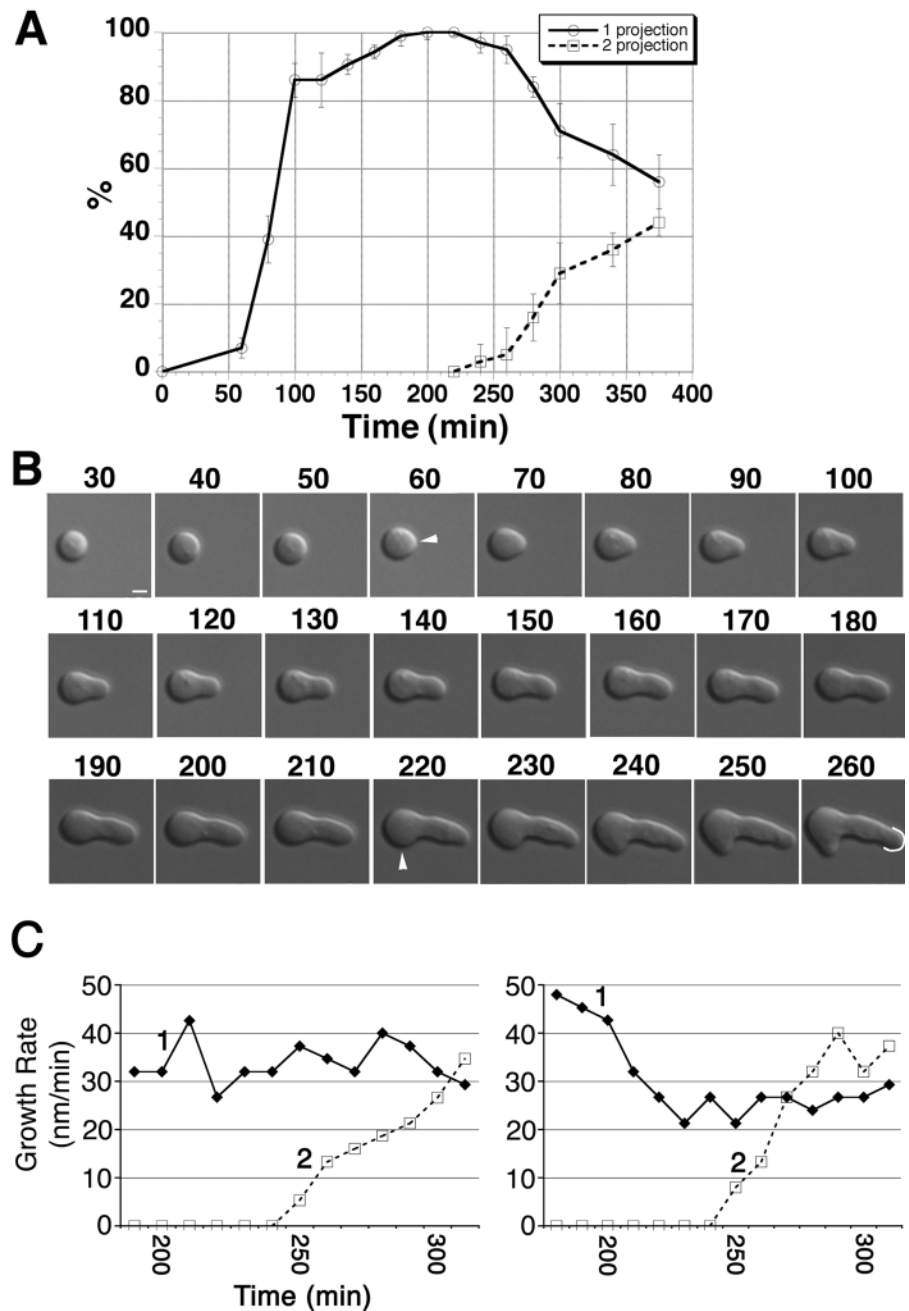
(Fig. 2 A). In these latter cases, the second site of actin polarization was usually present as a broad region on the cell surface that was not associated with a visible projection (Fig. 2 A, arrow), suggesting that these sites represented presumptive projection sites or the earliest stages of projection growth. Interestingly, cells without polarized actin sites were not observed. Taken together, our results suggest that old projections terminate growth at approximately the same time or almost immediately following the initiation of new projections.

Transient disruption of the actin cytoskeleton promotes projection initiation

The tight temporal linkage between termination of mating projection growth and initiation of a new projection suggests that the termination of projection growth may promote the initiation of a new projection. As noted in the Introduction, disruption of the actin cytoskeleton is expected to block polarized growth in a growing projection. We therefore tested whether a transient disruption of the actin cytoskeleton promotes the initiation of new projections. Wild-type cells were incubated with α-factor for 120 min, when >85% of the cells had formed one projection. The cells were then treated with the actin polymerization inhibitor latrunculin A (Lat-A) for 5 min in order to disrupt the actin cytoskeleton, washed in the presence of α-factor, and returned to growth in the presence of α-factor for an additional 95 min. Analysis of the actin cytoskeleton after Lat-A treatment confirmed that >95% of the cells had no visible actin polarization. Lat-A–treated cells formed more projections (1.71 ± 0.09) than mock-treated control cells (1.38 ±

0.07), indicating that disruption of the actin cytoskeleton promotes the initiation of new projections (Fig. 2 B). At 95 min after removal of Lat-A, the cells never had more than two projections (presumably the existing one and a new one), indicating that multiple projections were not forming simultaneously. Thus, Lat-A–induced transient disruption of the actin cytoskeleton promotes the initiation of new projections in wild-type cells.

Deletion of genes encoding the polarisome components Spa2, Pea2, or Bni1 decreases the frequency of mating projection formation

We next wished to identify molecular components important for controlling the timing of projection formation. *cdc34-2* strains grown at the restrictive temperature arrest with low mitotic Cdk activity and form multiple buds with a regular periodicity (Goebl et al., 1988). Preliminary observations previously indicated that *spa2 cdc34-2* cells do not initiate a second bud (Bidlingmaier and Snyder, 2002), suggesting that Spa2 may be a component of the unknown oscillatory mechanism that generates periodic initiation of polarized growth in *cdc34-2* and pheromone-treated cells. Spa2 is a component of the "polarisome," a multiprotein complex that is important for polarized growth (Sheu et al., 1998). To determine if Spa2 is important for periodic mating projection formation, we treated *spa2Δ* cells with α-factor and measured the timing of projection emergence (Fig. 3 A). The formation of the first projection is slightly delayed in *spa2Δ* cells. The time at which 50% of *spa2Δ* cells had formed one projection was 85 min, as compared with 67 min for wild-type cells (Fig. 3 A). The emergence of second projections in *spa2Δ* cells was severely delayed relative to wild-type cells. After 375 min of α-factor treatment, only 40% of *spa2Δ* cells had formed a second projection (Fig. 3 A). In contrast, 50% of wild-type cells had formed a second projection by 210 min (Fig. 1 A). *spa2Δ* cells had an average initiation period of 201 ± 13 min (compared with 119 ± 4 for wild-type cells). Projection morphology and growth rate were also affected in *spa2Δ* cells. The projections formed by *spa2Δ* cells were on average 60% wider than wild-type projections (2.4 ± 0.2 vs. 1.5 ± 0.1 μm, respectively), and the average total extension rate for *spa2Δ* projections was almost three times greater than the wild-type extension rate (42.7 ± 2.7 vs. 16.1 ± 0.8 nm/min, respectively).

To examine this phenotype more closely in individual cells, *spa2Δ* cells were treated with pheromone and analyzed by time-lapse microscopy (Fig. 3 B). In *spa2Δ* cells, the first projections became visible after ∼60 min of pheromone treatment, and the average time at which cells formed their first projection was 75 ± 12 min (n = 23). The average period between formation of the first and second projections was 174 ± 11 min (n = 11). The average projection growth rate was 32.0 ± 3.3 nm/min for first projections, and 29.9 ± 5.4 nm/min for second projections (n = 8). The discrepancy between the average total extension rate and the average extension rate of individual projections is due to the fact that first projections continue to grow for an extended period of time after the emergence of the second projection (see next section). Thus, *spa2Δ* cells initiate pro-
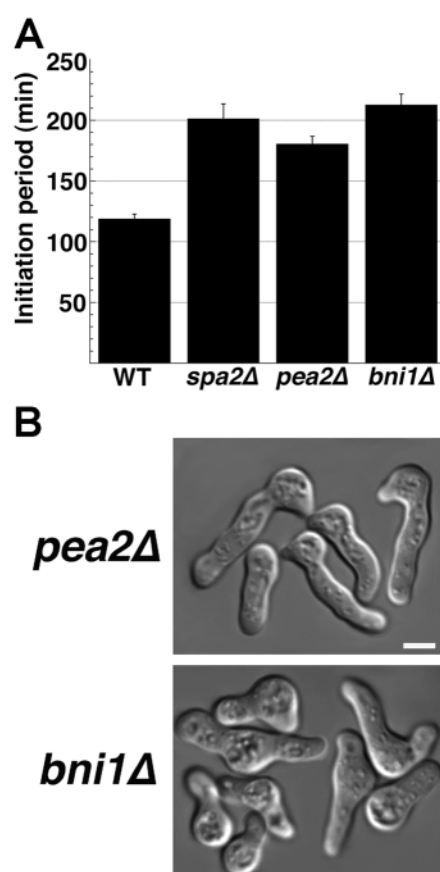

Figure 4.   **Deletion of *PEA2* or *BNI1* decreases the frequency of mating projection initiation.** (A) Mating projection initiation period of wild-type, *spa2Δ*, *pea2Δ*, and *bni1Δ* cells. Wild-type, *spa2Δ*, *pea2Δ*, and *bni1Δ* cells were incubated with α-factor for 6 h, and the average time per mating projection initiation was calculated. At least 100 cells were analyzed for each strain and the data represent the average of at least two independent experiments. (B) *pea2Δ* and *bni1Δ* cells after a 6-h treatment with α-factor. Bar, 3.0 μm.

jections less frequently than wild-type cells and form wider, faster growing projections.

Other known polarisome components include Pea2 and Bud6, whose molecular functions are unknown, and the formin homologue Bni1, which has recently been shown to promote the assembly of actin filaments (Evangelista et al., 2002; Sagot et al., 2002; Pring et al., 2003). To determine if Pea2, Bud6, or Bni1 are important for the frequency of periodic mating projection initiation, we treated *pea2Δ*, *bud6Δ*, and *bni1Δ* cells with α-factor for 6 h and counted the total number of projections formed to determine the initiation period. Examination of intermediate time points confirmed that projections emerged sequentially in all cases (unpublished data). Similar to *spa2Δ* cells, *pea2Δ* and *bni1Δ* cells had initiation periods that are significantly longer than the wild-type initiation period (180 ± 7 and 213 ± 9 min, respectively, vs. 119± 4 for wild type; Fig. 4 A) and formed projections that are wider than wild-type projections (Fig. 4 B). Deletion of *BUD6* did not affect the frequency of mating projection formation or the morphology of the projections (unpublished data). We also analyzed the rate of projection growth in *pea2Δ* and *bni1Δ* cells. Similar to *spa2Δ*

Figure 5. **Delocalization of actin is delayed in *spa2Δ*, *pea2Δ*, and *bni1Δ* cells.** (A) *spa2Δ*, *pea2Δ*, and *bni1Δ* cells were incubated with α-factor for 6 h and stained for F-actin. Fields containing cells with multiple projections were preferentially chosen to present actin staining in such cells. Bar, 3.0 μm. (B) The percentage of cells with two projections that had two polarized actin sites was determined. At least 150 cells were analyzed for each strain, and the data represent the average of two independent experiments. (C) *spa2Δ* cells were incubated with α-factor for 150 min and then treated with Lat-A to transiently disrupt the actin cytoskeleton. Cells were returned to growth in the presence of α-factor for 150 min, and the number of total projections formed was compared with mock-treated cells. At least 100 cells were analyzed for each time point, and the data represent the average of two independent experiments.
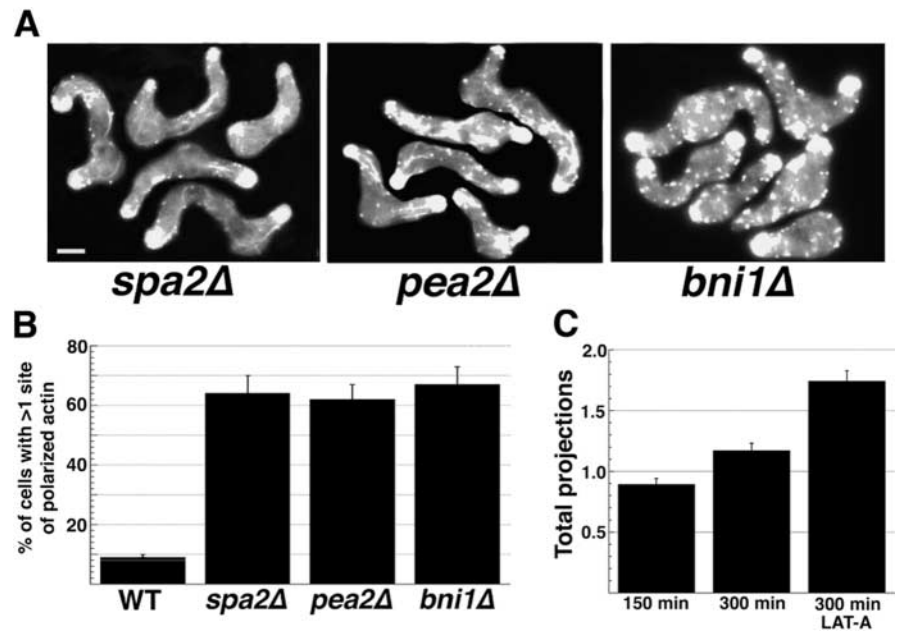
cells, the average total projection growth rate for *pea2Δ* cells was almost three times the rate of wild-type projection growth (47.3 ± 4.6 nm/min). The average total growth rate was lower for *bni1Δ* projections (27.6 ± 0.8 nm/min) but still greater than the wild-type total growth rate. Thus, similar to *spa2Δ* cells, *pea2Δ* and *bni1Δ* cells initiate mating projections less frequently than wild-type cells and form wider, faster growing projections.

Deletion of *SPA2*, *PEA2*, or *BNI1* delays termination of projection growth

We also examined the cessation of projection growth in *spa2Δ*, *pea2Δ*, and *bni1Δ* cells. Surprisingly, time-lapse analysis of *spa2Δ* cells revealed that in the majority of cases (92%, n = 13), growth of the first projection continues for >20 min after the emergence of a second projection (Fig. 3, B and C). Interestingly, the emergence of a second projection did not usually decrease the growth rate of the first projection. The average growth rate of the first projection after emergence of the second projection was 33.2 ± 8.9 nm/min, as compared with 32.0 ± 3.3 and 29.9 ± 5.4 nm/min average growth rates for first and second projections, respectively (n = 11). Thus, *spa2Δ* mutants are defective in termination of projection growth, and the initiation of the second projection does not compromise the growth rate of the first.

To investigate the growth termination phenotype further, we analyzed the actin cytoskeleton in pheromone-treated *spa2Δ*, *pea2Δ*, and *bni1Δ* cells. After a 6-h incubation with α-factor, >60% of *spa2Δ*, *pea2Δ*, and *bni1Δ* cells with two visible projections had actin polarized in the tips of both projections, indicating that they were growing simultaneously (Fig. 5, A and B). *spa2Δ* and *pea2Δ* projections also had actin cables; these were absent or difficult to detect in *bni1Δ* projections (Fig. 5 A). Thus, in addition to their importance in periodic mating projection initiation, Spa2, Pea2, and Bni1 are important for actin delocalization and growth termination.

To determine if transient disruption of the actin cytoskeleton accelerates the initiation of new projections in *spa2Δ* cells, we incubated *spa2Δ* cells with α-factor for 150 min, when >85% had formed one projection. The cells were then treated with the actin polymerization inhibitor Lat-A for 5 min in order to disrupt the actin cytoskeleton, washed in the presence of α-factor, and returned to growth in the presence of α-factor for 145 additional minutes. Analysis of the actin cytoskeleton just after Lat-A treatment confirmed that >95% of the cells had no visible actin polarization (unpublished data). Lat-A–treated *spa2Δ* cells formed more total projections (1.74 ± 0.09) than mock-treated *spa2Δ* cells (1.17 ± 0.06), indicating that disruption of the actin cytoskeleton promotes the initiation of new projections (Fig. 5 C). First projections appeared to stop growing after Lat-A treatment because most cells contained small projections; *spa2Δ* cells would normally have much longer projections for the same incubation period. Thus, the transient disruption of the actin cytoskeleton promotes the initiation of new projections in *spa2Δ* cells.

Regulators of Cdc42 activity control the frequency of projection initiation in a Bni1-dependent manner

As Bni1 is a downstream effector of the small GTPase Cdc42, we wished to determine if Cdc42 is important for periodic mating projection initiation. We attempted to determine if Cdc42 activity regulates the periodicity of mating projection formation by analyzing cells containing the hyperactive *cdc42^{G60D}* allele, which causes cells to produce multiple buds that grow simultaneously (Caviston et al., 2002). However, the analysis was complicated by the fact that although cells arrested, most lysed after a 5-h α-factor treatment, and multibudded cells (∼50% of population) did not appear to undergo a morphological response to pheromone (unpublished data).

cdc42^{G60D} cells have dramatically elevated levels of GTP-bound Cdc42 (Caviston et al., 2002); we therefore deter-

A

B

spa2Δ bem3Δ   pea2Δ bem3Δ   bni1Δ bem3Δ

C
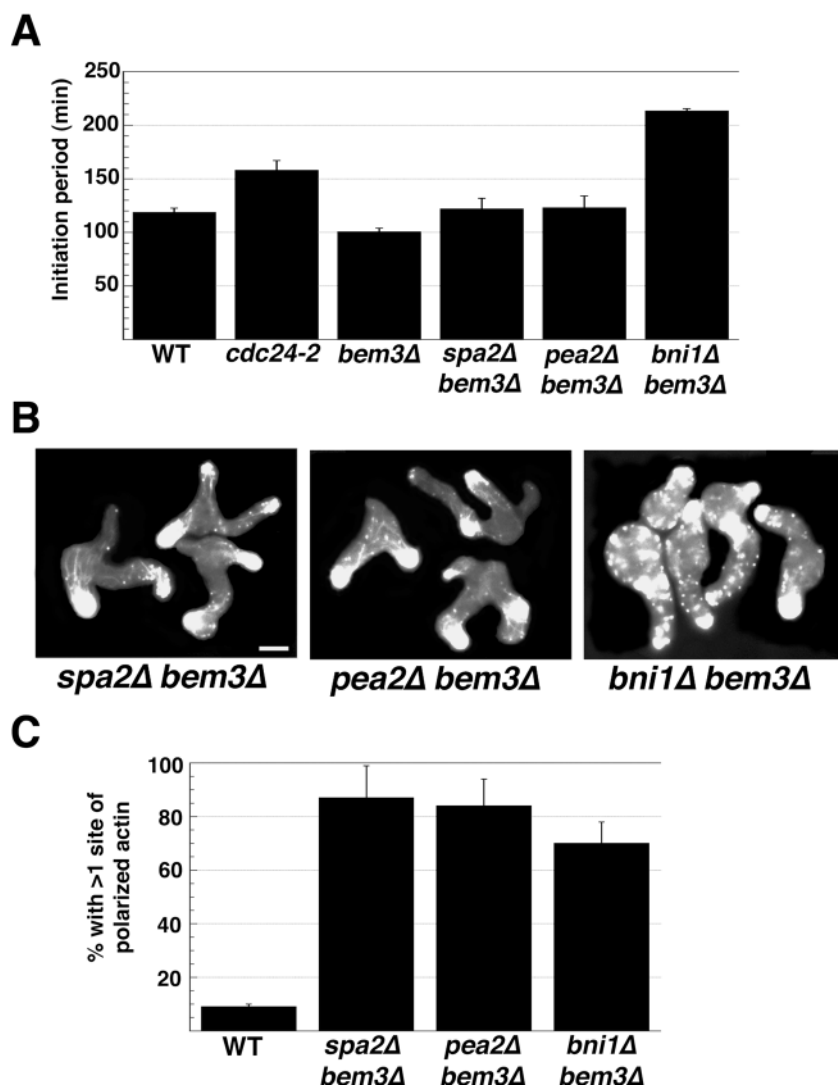
Figure 6. **Regulators of Cdc42 activity control the frequency of projection initiation in a Bni1-dependent manner.** (A) Mating projection initiation period of tested strains. Cells were incubated with α-factor for 6 h, and the average period between mating projection initiations was calculated. At least 100 cells were analyzed for each strain, and the data represent the average of at least two independent experiments. (B) spa2Δ bem3Δ, pea2Δ bem3Δ, and bni1Δ bem3Δ cells were incubated with 5 μg/ml α-factor for 6 h and stained for F-actin. Bar, 3.0 μm. (C) Percentage of cells with more than one site of polarized actin. Wild-type, spa2Δ bem3Δ, pea2Δ bem3Δ, and bni1Δ bem3Δ cells were incubated with α-factor for 6 h, and the percentage of cells with more than one polarized actin site was determined. At least 150 cells were analyzed for each strain, and the data represent the average of two independent experiments.

mined if more subtle changes in Cdc42 activity would affect the timing of mating projection initiation. Cdc42 is positively regulated by the GEF Cdc24 (Zheng et al., 1994) and negatively regulated by the GAPs Bem3, Rga1, and Rga2 (Smith et al., 2002). We analyzed projection formation in pheromone-treated *cdc24-2*, *bem3Δ*, *rga1Δ*, and *rga2Δ* cells. At the permissive temperature of 25°C, the projection initiation period of pheromone-treated *cdc24-2* cells was similar to wild-type cells (unpublished data). However, at the semipermissive temperature of 30°C, *cdc24-2* cells had a longer projection initiation period than wild-type cells (158 ± 9 vs. 119 ± 4 min, respectively; Fig. 6 A). In contrast, *bem3Δ* cells had a shorter projection initiation period than wild-type cells (101 ± 4 min; Fig. 6 A). The differences between the projection initiation periods of *cdc24-2* and *bem3Δ* cells and wild-type cells were statistically significant (P < 0.001 in both cases). The morphological response to pheromone was unaffected in *rga1Δ* and *rga2Δ* cells (unpublished data). Notably, >90% of *cdc24-2* and *bem3Δ* cells had only one polarized actin site, indicating that growth termination was not affected in these mutants. The average total projection growth rate in *bem3Δ* and *cdc24-2* cells (16.3 ± 1.3 and 15.0 ± 1.1 nm/min, re-

spectively) was also similar to wild type, indicating that the timing alterations were not due to general effects on cell growth. Thus, Bem3 and Cdc24 regulate the frequency of periodic mating projection initiation.

We next tested the effect of deleting *BEM3* in *spa2Δ*, *pea2Δ*, and *bni1Δ* cells. Deletion of *BEM3* increased the frequency of projection initiation to near wild-type levels in both *spa2Δ* and *pea2Δ* cells. The projection initiation periods of *spa2Δ bem3Δ* and *pea2Δ bem3Δ* cells were 122 ± 10 and 123 ± 11 min, respectively (Fig. 6 A). However, deletion of *BEM3* had no effect on projection initiation frequency in *bni1Δ* cells (Fig. 6 A). Significantly, after a 6-h treatment with α-factor, the projections formed by *spa2Δ bem3Δ* and *pea2Δ bem3Δ* cells were longer than wild-type projections, and >60% of *spa2Δ bem3Δ* and *pea2Δ bem3Δ* cells had two or more polarized actin sites, indicating that the actin delocalization and growth termination defects of *spa2Δ* and *pea2Δ* cells are not suppressed by deletion of *BEM3* (Fig. 6, B and C). As deletion of *BEM3* increases the frequency of projection initiation, but not growth termination, it is likely that the frequency of projection initiation and termination is regulated by partially separate pathways. Thus, our results suggest that the Cdc42 regulators Bem3
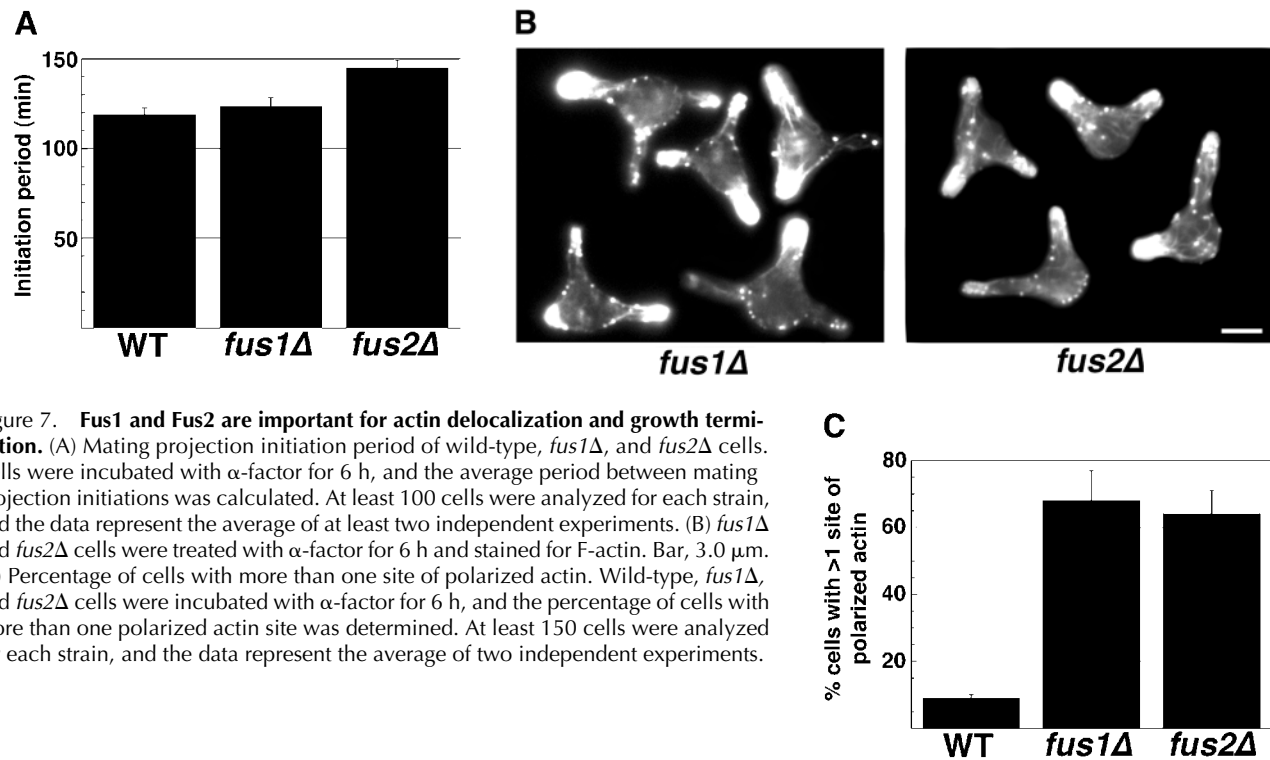
Figure 7. **Fus1 and Fus2 are important for actin delocalization and growth termination.** (A) Mating projection initiation period of wild-type, *fus1Δ*, and *fus2Δ* cells. Cells were incubated with α-factor for 6 h, and the average period between mating projection initiations was calculated. At least 100 cells were analyzed for each strain, and the data represent the average of at least two independent experiments. (B) *fus1Δ* and *fus2Δ* cells were treated with α-factor for 6 h and stained for F-actin. Bar, 3.0 μm. (C) Percentage of cells with more than one site of polarized actin. Wild-type, *fus1Δ*, and *fus2Δ* cells were incubated with α-factor for 6 h, and the percentage of cells with more than one polarized actin site was determined. At least 150 cells were analyzed for each strain, and the data represent the average of two independent experiments.

and Cdc24 regulate the frequency of periodic mating projection formation. Furthermore, Bem3 acts upstream of Bni1.

Fus1 is important for the termination of projection growth but not the frequency of projection initiation

A screen for genes required for mating in chemotropism-defective cells identified a small set of genes that includes *SPA2*, *PEA2*, *BNI1*, *FUS1*, and *FUS2* (Dorer et al., 1997). Transcription of both *FUS1* and *FUS2* is dramatically up-regulated in response to pheromone (Trueheart et al., 1987), and *fus1Δ* and *fus2Δ* mutants have cell fusion defects that are similar to those observed in *spa2Δ* mutants (Gammie et al., 1998). These similarities led us to investigate the effect of deleting *FUS1* and *FUS2* on the timing of mating projection initiation and termination in pheromone-treated cells. We incubated *fus1Δ* and *fus2Δ* cells with α-factor for 6 h and analyzed projection formation and actin distribution. The projection initiation period in *fus1Δ* cells was not significantly different from wild-type cells (124 ± 5 min) (Fig. 7 A). However, growth termination was severely delayed; *fus1Δ* projections grew to greater lengths than wild-type projections, and 68% of cells had more than one site of polarized actin (Fig. 7, B and C). Thus, Fus1 is important for growth termination and delocalization of actin patches. In *fus2Δ* cells, the initiation period was slightly increased (145 ± 4 min) (Fig. 7 A), although much less than in polarisome mutants. Growth termination was also delayed in *fus2Δ* cells; 64% of cells had more than one site of polarized actin, and the projections grew to greater lengths than wild-type projections (Fig. 7, B and C). These results indicate that Fus1 and Fus2 are important for actin delocalization and the termination of projection growth. The observation that the frequency of mating projection initiation is not affected in

fus1Δ cells further supports the idea that the frequency of projection initiation and termination is regulated by partially separate pathways.

Deletion of *PHO85*, *SLT2*, or *CLA4* does not affect periodic mating projection initiation or delocalization of actin at projection growth sites

We also analyzed mutants for three other genes that have been implicated in cell morphogenesis: *PHO85*, *SLT2*, and *CLA4*. Although Cdc28 Cdk activity is not responsible for the periodic initiation of mating projections (Haase and Reed, 1999), yeast possess another Cdk, Pho85, that has been shown to play a role in morphogenesis and have some overlapping function(s) with Cdc28 (Lenburg and O'Shea, 2001). The mitogen-activated protein kinase Slt2 is important for cell integrity during polarized growth (Mazzoni et al., 1993; Zarzov et al., 1996). In α-factor–treated cells, Slt2 kinase activity rises at approximately the same time as the emergence of the first mating projection, and Slt2 kinase activity decreases just before the initiation of second projections and then rises again with the emergence of the second projection (Buehrer and Errede, 1997). The PAK-like kinase Cla4 is a Cdc42 effector and has been proposed to be part of a negative feedback loop that acts to down-regulate Cdc24 and turn off polarized growth (Gulli et al., 2000).

To determine if Pho85, Slt2, and Cla4 are important for periodic mating projection initiation or mating projection growth termination, we analyzed α-factor–treated *pho85Δ*, *slt2Δ*, and *cla4Δ* cells. For *slt2Δ* cells, the experiments were performed in the presence of 1 M sorbitol to prevent cell lysis. In each mutant strain, the frequency of mating projection formation was unaffected (unpublished data). The termination of growth (as determined by projection size) and

the delocalization of actin patches was also unaffected (unpublished data). Thus, Pho85, Slt2, and Cla4 do not appear to be important for periodic mating projection initiation or mating projection growth termination.

Discussion

The polarisome components Spa2, Pea2, and Bni1 regulate the frequency of periodic mating projection and are important for growth termination

In this report, we demonstrate that deletion of the genes encoding the polarisome components Spa2, Pea2, or Bni1 decreases the frequency of periodic mating projection formation in haploid cells treated with a high concentration of pheromone. Spa2 and Pea2 may act together to enhance the activity of Bni1, possibly by helping to localize or maintain Bni1 at polarized growth sites (Fig. 8). Consistent with this hypothesis, *spa2Δ pea2Δ*, *spa2Δ bni1Δ*, and *pea2Δ bni1Δ* double mutants do not have additive projection initiation frequency defects.

Surprisingly, our results indicate that Spa2, Pea2, and Bni1 are also important for actin delocalization and the termination of mating projection growth; projections grow to extreme lengths, and cells with two actively growing projections are frequently observed in these mutants. Interestingly, the projection growth rate is greatly increased in *spa2Δ* and *pea2Δ* mutants. Thus, the polarisome appears to both positively and negatively regulate polarized growth during periodic projection formation.

The cell fusion proteins Fus1 and Fus2 are important for projection growth termination

We have shown that growth termination and actin delocalization are also delayed in *fus1Δ* and *fus2Δ* cells. The expression of *FUS1* and *FUS2* is dramatically induced in response to pheromone, and Fus1 and Fus2 localize to the tips of mating projections and are important for the degradation of cell wall in the cell-fusion zone (McCaffrey et al., 1987; Trueheart et al., 1987; Elion et al., 1995; Gammie et al., 1998). Significantly, the frequency of periodic mating projection initiation is unaffected in *fus1Δ* cells. Pheromone induction of *FUS1* expression is normal in polarisome mutants (Sheu et al., 1998; Roberts et al., 2000), and overexpression of *FUS1* using a high-copy plasmid did not suppress the growth termination defects of polarisome mutants, suggesting that reduced expression of *FUS1* is not the cause of growth termination defects in polarisome mutants. Fus1 is a transmembrane protein with an intracellular SH3 domain (Trueheart et al., 1987; Trueheart and Fink, 1989) and interacts with actin in a two-hybrid assay (Uetz et al., 2000). It is possible that Fus1 concentrated in projection tips acts to locally destabilize the actin cytoskeleton, leading to growth termination.

Cdc42 may control the frequency of projection initiation by regulating the activity of Bni1

We have shown that the Cdc42 GAP, Bem3, and the Cdc42 GEF, Cdc24, regulate the frequency of periodic mating projection. Pheromone-treated *cdc24-2* cells have increased pro-
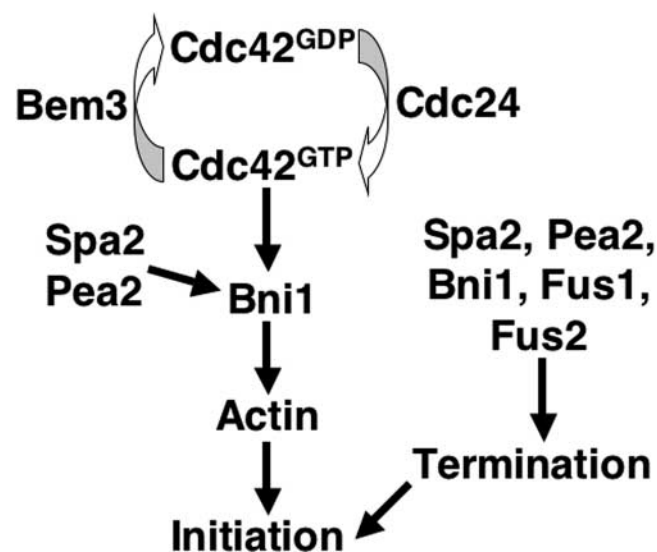

Figure 8. **Model of periodic mating projection initiation and termination (see Discussion).** Cdc42-GTP levels are regulated by the GEF, Cdc24, and the GAP, Bem3. Cdc42-GTP activates Bni1, which in turn promotes reorganization of the actin cytoskeleton, leading to projection initiation. Spa2 and Pea2 enhance the activity of Bni1. Spa2, Pea2, Bni1, Fus1, and Fus2 are important for the termination of projection growth.

jection initiation periods relative to wild-type cells at the semipermissive temperature of 30°C, while *bem3Δ* cells have a decreased initiation period. These results suggest that Cdc42-GTP levels may regulate projection initiation frequency. Deletion of *BEM3* suppresses the projection initiation frequency defects of *spa2Δ* and *pea2Δ* cells, but not *bni1Δ* cells. It is likely that deletion of *BEM3* results in higher levels of GTP-bound Cdc42, which in turn binds and activates Bni1 (Fig. 8). Thus, increased Bni1 activity caused by deletion of *BEM3* may be sufficient to compensate for the loss of Spa2 or Pea2 function.

Bni1 is probably not the only Cdc42-GTP effector important for projection initiation, as *bni1Δ* cells still form projections, albeit at reduced frequency. Presumably additional effectors also exist; candidates include Bnr1, a homologue of Bni1, and Arp2/3 (Imamura et al., 1997; Lechler et al., 2001).

Interestingly, Cdc42 activity does not appear to affect projection growth termination; *cdc24-2* cells incubated with pheromone at the semirestrictive temperature form normal length projections and depolarize actin, and deletion of *BEM3* does not suppress the projection growth termination and actin delocalization defects of *spa2Δ* and *pea2Δ* cells. Thus, it is likely that the frequency of projection initiation and termination is regulated by partially separate pathways. Consistent with this, Fus1 is important for projection growth termination but not initiation frequency (Fig. 8).

Model for periodic mating projection initiation

Our results indicate that the polarisome and Cdc42 regulators control the frequency of periodic mating projection initiation. We propose a model in which periodic mating projection initiation is driven by oscillating levels of Cdc42-GTP in the cell periphery. Initially, a low level of Cdc42-GTP is

evenly spread throughout the plasma membrane. Exposure to pheromone stimulates the export of Cdc24 from the nucleus to activated receptors at the cell surface. The GEF activity of Cdc24 causes Cdc42-GTP levels to rise. In the absence of a pheromone gradient, Cdc42-GTP levels initially rise evenly throughout the plasma membrane. It has recently been reported that a sufficient concentration of Cdc42-GTP at the cell surface can promote actomyosin-dependent spontaneous generation of polarity (Wedlich-Soldner et al., 2003). The authors propose that a critical local concentration of Cdc42-GTP on the plasma membrane can produce a positive feedback loop in which Cdc42-GTP–induced actin polymerization increases the probability of further Cdc42 accumulation to that site (Wedlich-Soldner et al., 2003). Our results are consistent with this model and further suggest that Bni1, facilitated by Spa2 and Pea2, is an important downstream effector of Cdc42-GTP that promotes the initiation of mating projections. Thus, once a critical local threshold of Cdc42-GTP is reached, an actin-dependent positive feedback is established, leading to polarization of secretion and clustering of receptors and growth machinery at the projection tip. As a result of this polarization, we propose that a critical rate-limiting factor, or factors, is depleted from the remaining plasma membrane. Potential candidates for these factors include Cdc42 and pheromone receptor. As a result of the depletion of critical factors, the concentration of Cdc42-GTP in the remaining plasma membrane drops below the critical threshold for initiation. In the continuing presence of pheromone, Cdc42-GTP levels rise throughout the cell periphery until the critical threshold concentration is reached again, resulting in the initiation of the next mating projection. We attempted to detect oscillations in the level of Cdc42-GTP in cells undergoing periodic mating projection formation; however, our assays were not able to reliably detect Cdc42-GTP in pheromone-treated cells. Methods for detecting the quantity and location of Cdc42-GTP in individual cells may be required to detect Cdc42-GTP oscillations.

This model provides a framework for understanding many of our observations. Mutants that affect Cdc42-GTP levels (such as *bem3Δ* and *cdc24-2*) would change the time it takes cells to reach the critical threshold for initiation. As *spa2Δ* and *pea2Δ* mutants are expected to have reduced Bni1 activity, and thus require higher local concentrations of Cdc42-GTP for initiation, the refractory period between projection initiations will be increased in these mutants.

Relationship between initiation and termination of projection growth

During the cell cycle, the initiation of many events is dependent upon the completion of a previous event. In the case of periodic projection formation, it is possible that the initiation of a new projection is delayed until the previous projection has terminated growth. Our time-lapse observations and actin staining of wild-type cells treated with high concentration of pheromone indicate that termination of projection growth occurs almost immediately ($\sim$10 min) following the initiation of new projections. Additionally, after the emergence of the first projection, cells without polarized actin are not observed. Thus, it appears that old projections do not completely terminate growth before the

initiation of the next projection. It is possible that growth termination begins before the initiation of the next projection but is not completed until after the emergence of the next projection. However, in polarisome, *fus1Δ*, and *fus2Δ* mutants, previous projections continue to grow well after new projections have initiated. Thus, the termination of old projections does not appear to be a strict prerequisite for the initiation of new projections.

Our results suggest that projection initiation and termination are regulated by partially separate pathways and that the termination of the previous projection is not required for the initiation of the next projection. Nevertheless, there appears to be a relationship between projection termination and initiation. Lat-A–induced termination of projection growth promotes the initiation of new projections in both wild-type and *spa2Δ* cells (Fig. 8). Perhaps the disassembly of projection growth sites releases an essential factor, or factors, that is rate limiting for the initiation of new projections. Why do the timing of initiation and termination appear to be tightly linked in wild-type cells? Perhaps the frequency of termination may be naturally close to the frequency of initiation in wild-type cells. If growth termination begins before the initiation of the next projection, the accompanying release of critical factors may promote the initiation of a new projection.

Biological significance of periodic mating projection initiation and termination

The ability of cells to orient projection growth along a pheromone gradient (chemotropism) allows mating cells to efficiently seek out a partner and position projection tips in preparation for cell fusion (Madden and Snyder, 1992; Erdman et al., 1998). In the presence of a high isotropic concentration of pheromone, cells execute a response termed default mating (Dorer et al., 1997). Interestingly, Spa2, Pea2, Bni1, Fus2, and Fus1 are important for default mating (Dorer et al., 1997). It has been suggested that default mating places a more stringent requirement on cell fusion than chemotropic mating (Dorer et al., 1997).

We propose that in the absence of a pheromone gradient to direct projection growth toward a nearby partner, periodic mating projection initiation may allow cells to probe in different directions for a partner. In *spa2Δ*, *pea2Δ*, and *bni1Δ* mutants, this probing may be less efficient because projections initiate less frequently and continue to grow in the same direction for long periods of time. Thus, periodic mating projection formation cycles may be an important biological response that facilitates efficient mating in the presence of a saturating concentration of pheromone.

Interestingly, our results indicate that *spa2Δ*, *pea2Δ*, *bni1Δ*, *fus1Δ*, and *fus2Δ* mutants share another common defect in projection growth termination. New cell wall must be continuously synthesized at the tips of growing projections to maintain cell integrity. However, cell wall material between mating cells must be removed before fusion can occur. Thus, delayed projection growth termination may contribute to the cell fusion defects observed in these mutants. In addition, it is also possible that the presence of more than one actively growing projection interferes with the process of mating.

Table I. **Yeast strains used in this study**

Strain	Genotype	Source
Y3000	*MAT**a** bar1Δ::LEU2 leu2Δ98 ura3-52 lys2-801 ade2-101 his3-Δ200*	This study
Y3001	*MAT**a** spa2Δ::HIS3 bar1Δ::LEU2 leu2Δ98 ura3-52 lys2-801 ade2-101 his3-Δ200*	This study
Y3002	*MAT**a** pea2Δ::URA3 bar1Δ::LEU2 leu2Δ98 ura3-52 lys2-801 ade2-101 his3-Δ200*	This study
Y3003	*MAT**a** bni1Δ::URA3 bar1Δ::LEU2 leu2Δ98 ura3-52 lys2-801 ade2-101 his3-Δ200*	This study
Y3005	*MAT**a** bem3Δ::HIS3 bar1Δ::LEU2 leu2Δ98 ura3-52 lys2-801 ade2-101 his3-Δ200*	This study
Y3008	*MAT**a** cdc24-2 bar1Δ::LEU2 leu2Δ98 ura3-52 lys2-801 ade2-101 his3-Δ200*	This study
JPC241	*MAT**a** cdc42^{G60D} trp1 leu2 ura3 his3 lys2*	E. Bi
Y3009	*MAT**a** spa2Δ::URA3 bem3Δ::HIS3 bar1Δ::LEU2 leu2Δ98 ura3-52 lys2-801 ade2-101 his3-Δ200*	This study
Y3010	*MAT**a** pea2Δ::URA3 bem3Δ::HIS3 bar1Δ::LEU2 leu2Δ98 ura3-52 lys2-801 ade2-101 his3-Δ200*	This study
Y3011	*MAT**a** bni1Δ::URA3 bem3Δ::HIS3 bar1Δ::LEU2 leu2Δ98 ura3-52 lys2-801 ade2-101 his3-Δ200*	This study
Y3012	*MAT**a** fus1Δ::URA3 bar1Δ::LEU2 leu2Δ98 ura3-52 lys2-801 ade2-101 his3-Δ200*	This study
Y3013	*MAT**a** fus2Δ::URA3 bar1Δ::LEU2 leu2Δ98 ura3-52 lys2-801 ade2-101 his3-Δ200*	This study

Materials and methods

Yeast strains and media

Yeast strains used in this study were congenic with S288c (Table I). Standard genetic methods and growth media were used as described previously (Guthrie and Fink, 1991). Deletions of the entire protein coding regions of *SPA2*, *PEA2*, *BNI1*, *BUD6*, *BEM3*, *RGA1*, *RGA2*, *FUS1*, *FUS2*, *CLA4*, *PHO85*, and *SLT2* were produced by the PCR method described by Baudin et al. (1993). Deletions were confirmed by PCR. The *cdc24-2* allele has been described previously (Sloat et al., 1981). The *cdc42^{G60D}* strain was provided by E. Bi (University of Pennsylvania, Philadelphia, PA) (Caviston et al., 2002).

Analysis of periodic mating projection initiation

For quantitative analysis of mating projection formation defects, early log phase cells were treated with 5 μg/ml α-factor (Sigma-Aldrich) for the indicated time periods and fixed with 3.7% formaldehyde. Images were recorded using a Leitz Aristoplan microscope and a Sensys charge-coupled device camera; subsequent image processing was done using Adobe PhotoShop software (Adobe Systems Inc.). F-actin was stained with rhodamine-conjugated phalloidin (Molecular Probes). Data were collected from captured images. The length and width of mating projections were measured from captured images using Imagepoint Lab Spectrum software (Signal Analytics). The average time per projection initiation, including the first (initiation period), was determined by dividing the time (usually 6 h) by the average number of projections formed. The significance of the differences between wild-type and *cdc24-2* and *bem3Δ* initiation periods was verified by *t* test analysis of population data. The average rate of total projection growth was calculated by dividing total projection length by time. At least 100 cells were analyzed for each time point/experiment, and the average of at least two experiments was calculated. Standard deviations were determined and presented as ±.

Time-lapse analysis of living α-factor–treated cells

To make YPAD/agarose pads, YPAD + 2% agarose was melted and 5 μg/ml α-factor was added. Several drops were placed on a microscope slide and covered with a coverslip. Cells were grown to log phase in YPAD, and α-factor was added at a concentration of 5 μg/ml. The coverslips were carefully removed, a drop of cells was added directly to the YPAD/agarose pad, and the cells were recovered with a coverslip. Images of the same field of cells were taken at 10-min intervals during the course of the experiments. Cells grown on the pads remained viable for at least 8 h. The timing of the emergence of first and second projections for multiple cells was determined from the time-lapse images. Projection growth (first and second) was measured for each 10-min interval, and a 30-min moving average was calculated and used to plot the growth rate as a function of time. An average over the entire period of growth for multiple cells was used to calculate the average growth rates of first projections (before and after second projection formation) and second projections. Standard deviations for the timing of projection formation and growth rates are indicated as ±.

Lat-A treatment of α-factor–treated cells

Exponentially growing cells were treated with 5 μg/ml α-factor until >85% had formed one mating projection. Cells were pelleted and resuspended in 50 μl YPAD + 5 μg/ml α-factor. Lat-A (Molecular Probes) was added from a 10 mM DMSO stock to a final concentration of 200 μM. After 5 min, the cells were washed three times with YPAD + 5 μg/ml α-factor and returned to growth in YPAD + 5 μg/ml α-factor. Actin staining confirmed that the actin cytoskeleton had been disrupted in >95% of the cells. At the indicated times following Lat-A treatment, the cells were fixed, and the number of mating projections was analyzed. At least 100 cells were analyzed for each experiment; the average of two experiments was calculated and standard deviations are presented as ±.

References

Baudin, A., O. Ozier-Kalogeropoulos, A. Denouel, F. Lacroute, and C. Cullin. 1993. A simple and efficient method for direct gene deletion in *Saccharomyces cerevisiae*. *Nucleic Acids Res.* 21:3329–3330.

Bedinger, P.A., K.J. Hardeman, and C.A. Loukides. 1994. Travelling in style: the cell biology of pollen. *Trends Cell Biol.* 4:132–138.

Bidlingmaier, S., and M. Snyder. 2002. Large-scale identification of genes important for apical growth in *Saccharomyces cerevisiae* by directed allele replacement technology (DART) screening. *Funct. Integr. Genomics.* 1:345–356.

Bretscher, A. 2003. Polarized growth and organelle segregation in yeast: the tracks, motors, and receptors. *J. Cell Biol.* 160:811–816.

Bucking-Throm, E., W. Duntze, L.H. Hartwell, and T.R. Manney. 1973. Reversible arrest of haploid yeast cells in the initiation of DNA synthesis by a diffusible sex factor. *Exp. Cell Res.* 76:99–110.

Buehrer, B.M., and B. Errede. 1997. Coordination of the mating and cell integrity mitogen-activated protein kinase pathways in *Saccharomyces cerevisiae. Mol. Cell. Biol.* 17:6517–6525.

Caviston, J.P., S.E. Tcheperegine, and E. Bi. 2002. Singularity in budding: a role for the evolutionarily conserved small GTPase Cdc42p. *Proc. Natl. Acad. Sci. USA.* 99:12185–12190.

Chenevert, J., N. Valtz, and I. Herskowitz. 1994. Identification of genes required for normal pheromone-induced cell polarization in *Saccharomyces cerevisiae. Genetics.* 136:1287–1296.

Chun, K.T., and M.G. Goebl. 1997. Mutational analysis of Cak1p, an essential protein kinase that regulates cell cycle progression. *Mol. Gen. Genet.* 256: 365–375.

da Silva, J.S., and C.G. Dotti. 2002. Breaking the neuronal sphere: regulation of the actin cytoskeleton in neuritogenesis. *Nat. Rev. Neurosci.* 3:694–704.

Dorer, R., C. Boone, T. Kimbrough, J. Kim, and L.H. Hartwell. 1997. Genetic analysis of default mating behavior in *Saccharomyces cerevisiae. Genetics.* 146: 39–55.

Elion, E.A., J. Trueheart, and G.R. Fink. 1995. Fus2 localizes near the site of cell fusion and is required for both cell fusion and nuclear alignment during zygote formation. *J. Cell Biol.* 130:1283–1296.

Erdman, S., L. Lin, M. Malczynski, and M. Snyder. 1998. Pheromone-regulated genes required for yeast mating differentiation. *J. Cell Biol.* 140:461–483.

Evangelista, M., K. Blundell, M.S. Longtine, C.J. Chow, N. Adames, J.R. Pringle, M. Peter, and C. Boone. 1997. Bni1p, a yeast formin linking Cdc42p and the actin cytoskeleton during polarized morphogenesis. *Science.* 276:118–122.

Evangelista, M., D. Pruyne, D.C. Amberg, C. Boone, and A. Bretscher. 2002. Formins direct Arp2/3-independent actin filament assembly to polarize cell growth in yeast. *Nat. Cell Biol.* 4:260–269.

Fujiwara, T., K. Tanaka, A. Mino, M. Kikyo, K. Takahashi, K. Shimizu, and Y. Takai. 1998. Rho1p-Bni1p-Spa2p interactions: implication in localization of Bni1p at the bud site and regulation of the actin cytoskeleton in *Saccharomyces cerevisiae*. *Mol. Biol. Cell.* 9:1221–1233.

Gammie, A.E., V. Brizzio, and M.D. Rose. 1998. Distinct morphological phenotypes of cell fusion mutants. *Mol. Biol. Cell.* 9:1395–1410.

Gehrung, S., and M. Snyder. 1990. The *SPA2* gene of *Saccharomyces cerevisiae* is important for pheromone-induced morphogenesis and efficient mating. *J. Cell Biol.* 111:1451–1464.

Goebl, M.G., J. Yochem, S. Jentsch, J.P. McGrath, A. Varshavsky, and B. Byers. 1988. The yeast cell cycle gene *CDC34* encodes a ubiquitin-conjugating enzyme. *Science.* 241:1331–1335.

Gulli, M.P., M. Jaquenoud, Y. Shimada, G. Niederhauser, P. Wiget, and M. Peter. 2000. Phosphorylation of the Cdc42 exchange factor Cdc24 by the PAK-like kinase Cla4 may regulate polarized growth in yeast. *Mol. Cell.* 6:1155–1167.

Guthrie, C., and G.R. Fink. 1991. Guide to yeast genetics and molecular biology. *Methods Enzymol.* 194:1–863.

Haase, S.B., and S.I. Reed. 1999. Evidence that a free-running oscillator drives G1 events in the budding yeast cell cycle. *Nature.* 401:394–397.

Heintzelman, M.B., and M.S. Mooseker. 1992. Assembly of the intestinal brush border cytoskeleton. *Curr. Top. Dev. Biol.* 26:93–122.

Imamura, H., K. Tanaka, T. Hihara, M. Umikawa, T. Kamei, K. Takahashi, T. Sasaki, and Y. Takai. 1997. Bni1p and Bnr1p: downstream targets of the Rho family small G-proteins which interact with profilin and regulate actin cytoskeleton in *Saccharomyces cerevisiae*. *EMBO J.* 16:2745–2755.

Jackson, C.L., and L.H. Hartwell. 1990. Courtship in *S. cerevisiae*: both cell types choose mating partners by responding to the strongest pheromone signal. *Cell.* 63:1039–1051.

Johnson, D.I. 1999. Cdc42: an essential Rho-type GTPase controlling eukaryotic cell polarity. *Microbiol. Mol. Biol. Rev.* 63:54–105.

Lechler, T., G.A. Jonsdottir, S.K. Klee, D. Pellman, and R.J. Li. 2001. A two-tiered mechanism by which Cdc42 controls the localization and activation of an Arp2/3-activating motor complex in yeast. *J. Cell Biol.* 155:261–270.

Lenburg, M.E., and E.K. O'Shea. 2001. Genetic evidence for a morphogenetic function of the *Saccharomyces cerevisiae* Pho85 cyclin-dependent kinase. *Genetics.* 157:39–51.

Lew, D.J., and S.I. Reed. 1993. Morphogenesis in the yeast cell cycle: regulation by Cdc28 and cyclins. *J. Cell Biol.* 120:1305–1320.

Madden, K., and M. Snyder. 1992. Specification of sites for polarized growth in *Saccharomyces cerevisiae* and the influence of external factors on site selection. *Mol. Biol. Cell.* 3:1025–1035.

Madden, K., and M. Snyder. 1998. Cell polarity and morphogenesis in budding yeast. *Annu. Rev. Microbiol.* 52:687–744.

Mathias, N., S.L. Johnson, M. Winey, A.E. Adams, L. Goetsch, J.R. Pringle, B. Byers, and M.G. Goebl. 1996. Cdc53p acts in concert with Cdc4p and Cdc34p to control the G1-to-S-phase transition and identifies a conserved family of proteins. *Mol. Cell. Biol.* 16:6634–6643.

Mazzoni, C., P. Zarov, A. Rambourg, and C. Mann. 1993. The *SLT2* (*MPK1*) MAP kinase homolog is involved in polarized cell growth in *Saccharomyces cerevisiae*. *J. Cell Biol.* 123:1821–1833.

McCaffrey, G., F.J. Clay, K. Kelsay, and G.F. Sprague, Jr. 1987. Identification and regulation of a gene required for cell fusion during mating of the yeast *Saccharomyces cerevisiae*. *Mol. Cell. Biol.* 7:2680–2690.

Ozaki-Kuroda, K., Y. Yamamoto, H. Nohara, M. Kinoshita, T. Fujiwara, K. Irie, and Y. Takai. 2001. Dynamic localization and function of Bni1p at the sites of directed growth in *Saccharomyces cerevisiae*. *Mol. Cell. Biol.* 21:827–839.

Pollard, T.D., and G.G. Borisy. 2003. Cellular motility driven by assembly and disassembly of actin filaments. *Cell.* 112:453–465.

Pring, M., M. Evangelista, C. Boone, C. Yang, and S.H. Zigmond. 2003. Mechanism of formin-induced nucleation of actin filaments. *Biochemistry.* 42: 486–496.

Pruyne, D., and A. Bretscher. 2000. Polarization of cell growth in yeast. I. Establishment and maintenance of polarity states. *J. Cell Sci.* 113:365–375.

Roberts, C.J., B. Nelson, M.J. Marton, R. Stoughton, M.R. Meyer, H.A. Bennett, Y.D. He, H. Dai, W.L. Walker, T.R. Hughes, et al. 2000. Signaling and circuitry of multiple MAPK pathways revealed by a matrix of global gene expression profiles. *Science.* 287:873–880.

Sagot, I., S.K. Klee, and D. Pellman. 2002. Yeast formins regulate cell polarity by controlling the assembly of actin cables. *Nat. Cell Biol.* 4:42–50.

Schwob, E., T. Bohm, M.D. Mendenhall, and K. Nasmyth. 1994. The B-type cyclin kinase inhibitor p40SIC1 controls the G1 to S transition in *S. cerevisiae*. *Cell.* 79:233–244.

Segall, J.E. 1993. Polarization of yeast cells in spatial gradients of alpha mating factor. *Proc. Natl. Acad. Sci. USA.* 90:8332–8336.

Sheu, Y.J., B. Santos, N. Fortin, C. Costigan, and M. Snyder. 1998. Spa2p interacts with cell polarity proteins and signaling components involved in yeast cell morphogenesis. *Mol. Cell. Biol.* 18:4053–4069.

Sloat, B.F., A. Adams, and J.R. Pringle. 1981. Roles of the *CDC24* gene product in cellular morphogenesis during the *Saccharomyces cerevisiae* cell cycle. *J. Cell Biol.* 89:395–405.

Smith, G.R., S.A. Givan, P. Cullen, and G.F. Sprague, Jr. 2002. GTPase-activating proteins for Cdc42. *Eukaryot. Cell.* 1:469–480.

Snyder, M. 1989. The Spa2 protein of yeast localizes to sites of cell growth. *J. Cell Biol.* 108:1419–1429.

Snyder, M., S. Gehrung, and B.D. Page. 1991. Studies concerning the temporal and genetic control of cell polarity in *Saccharomyces cerevisiae*. *J. Cell Biol.* 114:515–532.

Trueheart, J., and G.R. Fink. 1989. The yeast cell fusion protein Fus1 is O-glycosylated and spans the plasma membrane. *Proc. Natl. Acad. Sci. USA.* 86: 9916–9920.

Trueheart, J., J.D. Boeke, and G.R. Fink. 1987. Two genes required for cell fusion during yeast conjugation: evidence for a pheromone-induced surface protein. *Mol. Cell. Biol.* 7:2316–2328.

Uetz, P., L. Giot, G. Cagney, T.A. Mansfield, R.S. Judson, J.R. Knight, D. Lockshon, V. Narayan, M. Srinivasan, P. Pochart, et al. 2000. A comprehensive analysis of protein-protein interactions in *Saccharomyces cerevisiae*. *Nature.* 403:623–627.

Valtz, N., and I. Herskowitz. 1996. Pea2 protein of yeast is localized to sites of polarized growth and is required for efficient mating and bipolar budding. *J. Cell Biol.* 135:725–739.

Wedlich-Soldner, R., S. Altschuler, L. Wu, and R. Li. 2003. Spontaneous cell polarization through actomyosin-based delivery of the Cdc42 GTPase. *Science.* 299:1231–1235.

Zahner, J.E., H.A. Harkins, and J.R. Pringle. 1996. Genetic analysis of the bipolar pattern of bud site selection in the yeast *Saccharomyces cerevisiae*. *Mol. Cell. Biol.* 16:1857–1870.

Zarzov, P., C. Mazzoni, and C. Mann. 1996. The *SLT2*(*MPK1*) MAP kinase is activated during periods of polarized cell growth in yeast. *EMBO J.* 15:83–91.

Zheng, Y., R. Cerione, and A. Bender. 1994. Control of the yeast bud-site assembly GTPase Cdc42. Catalysis of guanine nucleotide exchange by Cdc24 and stimulation of GTPase activity by Bem3. *J. Biol. Chem.* 269:2369–2372.